Received: 14 December 2021 | Revised: 15 March 2022 | Accepted: 10 April 2022

DOI: 10.1002/cbf.3705

RESEARCH ARTICLE

CELL BIOCHEMISTRY & FUNCTION WILEY

Dose-dependent dominance: How cell densities design stromal cell functions during soft tissue healing

Philipp Kuhn | Monika Bubel | Martina Jennewein | Silke Guthörl | Tim Pohlemann | Martin Oberringer

Department of Trauma-, Hand- and Reconstructive Surgery, Saarland University, Homburg, Germany

Correspondence
Martin Oberringer, Department of Trauma-, Hand- and Reconstructive Surgery, Saarland University, Kirrberger Strasse, Bldg 57, Homburg 66421, Germany.
Email: martin.oberringer@uks.eu

Present address
Philipp Kuhn, Städtisches Krankenhaus Pirmasens gGmbH, Klinik für Anästhesie, Intensivmedizin und Schmerztherapie, Pirmasens, Germany.

Abstract

Regular soft tissue healing relies on the well-organized interaction of different stromal cell types with endothelial cells. However, spatiotemporal conditions might provoke high densities of one special stromal cell type, potentially leading to impaired healing. Detailed knowledge of the functions of rivaling stromal cell types aiming for tissue contraction and stabilization as well as vascular support is mandatory. By the application of an in vitro approach comprising the evaluation of cell proliferation, cell morphology, myofibroblastoid differentiation, and cytokine release, we verified a density-dependent modulation of these functions among juvenile and adult fibroblasts, pericytes, and adipose-derived stem cells during their interaction with microvascular endothelial cells in cocultures. Results indicate that juvenile fibroblasts rather support angiogenesis via paracrine regulation at the early stage of healing, a role potentially compromised in adult fibroblasts. In contrast, pericytes showed a more versatile character aiming at angiogenesis, vessel stabilization, and tissue contraction. Such a universal character was even more pronounced among adipose-derived stem cells. The explicit knowledge of the characteristic functions of stromal cell types is a prerequisite for the development of new analytical and therapeutic approaches for impaired soft tissue healing. The present study delivers new considerations concerning the roles of rivaling stromal cell types within a granulation tissue, pointing to extraordinary properties of pericytes and adipose-derived stem cells.

KEYWORDS

adipose-derived stem cell, endothelial cell, fibroblast, pericyte, stromal cell, tissue repair, wound healing

1 | INTRODUCTION

The integrity of human soft tissue can be disturbed by different circumstances, such as surgical intervention, trauma, and systemic diseases. Although basic physiological mechanisms generally allow the repair of injured soft tissue to a sufficient degree, wound treatment is still a major issue in health care.[1] Insufficient methods to assess the actual tissue situation during chronic wound healing might lead to the choice of a nonoptimal therapy. To harmonize assessment and therapeutic options for soft tissue healing, the knowledge of functions and regulation principles of participating and rivaling cells needs further broadening.

The healing sequence consists out of four overlapping phases: hemostasis, inflammation, proliferation, and remodeling.[2] Subsequent to the debridement of the tissue by immunocompetent cells, local and invading cells of stromal origin, situated in the connective tissue of the dermis and subcutis, assure both tissue stability and revascularization. Besides microvascular endothelial cells (EC), especially nonvascular stromal cells (SC), namely fibroblasts (FB), pericytes (PC), and adipose-derived stem cells (ASC) are main players from the proliferation phase on. Within the arising granulation tissue cell density increases in the early stages of healing, but later on cell density decreases during tissue maturation.[3] In a granulation tissue, the different cell types could be understood as competitors, so that local high density of a certain SC type can lead to its dominance. Autologous donation of SC during tissue repair, a promising strategy with respect to ASC[4] and FB,[5] can produce a dominating cell type, too.

Beneficial functions of any SC type within a granulation tissue depend on the correct spatiotemporal availability and density. SC functions are diverse,[6,7] including paracrine signaling, provision of extracellular matrix, and tissue contraction. Moreover, the interplay of SC with EC accounts for angiogenesis, a functional vascular support and the integration of microvessels into the maturing tissue. SC–EC interaction depends on cell-to-cell as well as cell-to-matrix contact and on paracrine regulation. Besides interleukin-8, especially vascular endothelial growth factor (VEGF), interleukin-6 (IL-6), and CC-chemokine ligand 2/monocyte chemoattractant protein (MCP-1) play major roles in tissue repair associated inflammation and angiogenesis[8–10] and depend on local SC cell densities. In this context, the combination of VEGF, IL-6, and MCP-1 seems to be advantageous for angiogenesis.[11]

Positive effects of the different SC in a granulation rely on their fundamental characteristics. PC are in direct contact with microvascular EC and contribute to the regulation of angiogenesis,[12] capillary reorganization,[13] microvascular tone, and blood flow.[14] ASC are located in a perivascular niche within adipose tissue,[15] which is near the granulation site and thus allow ASC to invade. In vitro, a vessel stabilizing function of ASC was suggested.[16] FB might derive from a perivascular/periadventitial niche of larger vessels,[17] where they interact with EC,[18] indicating their general potential to function as mural cells.

Vasoactive cell functions require contractile forces,[19] which in turn are provided by α-smooth muscle actin (α-SMA) expression.[20] With respect to PC, contractile function regulates the vascular diameter in capillaries.[12] All SC types examined in this study are able to differentiate into an α-SMA expressing myofibroblastoid cell type.

Furthermore, contractile forces are important for establishing contraction in a granulation tissue.[21] Support of tissue contraction seems to be clear for differentiated FB,[22] but it remains speculative for α-SMA-positive PC[23] and ASC.[24]

Negative effects of a locally dominating SC type might occur, such as fibrotic development in the case of persisting myofibroblastoid cells, originating from FB[25] or PC.[6] Another negative effect on the healing process may be given by accumulating aged cells, as wound healing is generally affected by advancing age.[26] Similarly, this issue is also important to estimate the influence of donor age on healing improvement after autologous SC donation. We addressed this topic by analyzing potential effects of the biological age of SC by inclusion of FB from a juvenile (juvenile human fibroblasts [jFB]) and an adult (adult human fibroblasts [aFB]) donor. Another negative effect might occur on the basis of the malignant potential of mesenchymal stem cells[27]; this issue especially has to be considered for applications in regenerative medicine.

With respect to the similar fundamental functions of different SC types, we can hypothesize in a simplifying way that SC are functionally torn between tissue contraction and vascular support in a granulation tissue. In our model SC monocultures of jFB, aFB, PC, and ASC serve to analyze the tissue related aspects, whereas interaction of these SC with EC allows the analysis of vascular functions. The basic design of the in vitro experiments relied on a well-established coculture assay.[28] The application of two different

Significance statement

Soft tissue healing is a spatio-temporal scenario where cell proliferation and tissue contraction as well as angiogenesis and vessel stabilization are profound requirements. This tissue re-organization process therefore implies cell interactions that might be orchestrated by a cell density dependent modulation of cell functions. In our approach, we propose an in vitro coculture model where different stromal cell types like juvenile and adult fibroblasts, pericytes, and adipose-derived stem cells are analyzed according to their interaction with microvascular endothelial cells in different cell densities. With respect to cytokines relevant for tissue repair associated angiogenesis and inflammation like VEGF, IL-6, and MCP-1 as well as α-SMA expression along with myofibroblastoid differentiation, we show the fibroblasts' participation in tissue stabilization and contraction and the more versatile character of pericytes and adipose-derived stem cells during the healing process.

initial cell densities together with those cell densities increasing during cell proliferation over time allow an extensive monitoring of cell density effects.

We aimed (i) to identify and demonstrate different roles of the SC types more specifically than provided by current literature, and (ii) to clarify, whether specific SC functions are density dependent, with regard to a dominating SC type occurring in granulation tissue or subsequent to autologous donation.

The study results allow new insights into the distinct functions of different SC types and may serve for future development of more adequate tissue assessment methods and therapeutic approaches in the context of soft tissue healing.

2 | MATERIALS AND METHODS

2.1 | Cells and cell culture setups

Commercially available primary nonvascular SC and EC were cultured under standard incubator conditions (37°C, 5% CO_2/air) to obtain identical cryo-cultures for each type, stored in a master cell bank (MCB). aFB (no. 1210411; Provitro) were grown in fibroblast growth medium (FGM, no. 2010401; Provitro) and stored in the MCB in passage (P) 5; jFB (no. C-12300; Promocell) were cultured in FGM and stored in P6; human PC (no. C-12980; Promocell) were grown in pericyte growth medium (no. C-28040; Promocell) and stored in P4, human mesenchymal stem cells from adipose tissue (ASC, no. C-12978; Promocell) were cultured in mesenchymal growth medium (no. C-28009; Promocell) and stored in P4, and juvenile human dermal microvascular EC (no. C-12210; Promocell) were cultured in endothelial cell growth medium (ECG, no. C-22020; Promocell) and stored in P6. Cryopreserved cells were thawed and expanded for the following experiments. Typical cell morphologies are shown Figure 1A.

We chose for a high density (HD) setup and an ultrahigh density (UHD) setup, the latter representing approximately doubled SC densities at the start of the experiment (Day 0). We observed the cells for another 2 days to identify shifts of the analytical parameters over time, delivering new insights for a transfer to the in vivo situation of a dynamic granulation tissue and a situation subsequent to cell donation.

To obtain similar cell densities of the SC types within each setup at the start, cells were seeded 48 h before with the required individual cell density, which was calculated on the basis of actual cell numbers determined by Casy cell counter (OLS OMNI Life Science) during passaging. All four different SC types were seeded on pretreated glass slides in quadruplicate ($4 \times 4 = 16$ cultures per experiment) in the dedicated media. After 24 h of cell attachment, medium was switched to individual coculture media, composed of one part of the individual SC medium and one part of ECG.

On Day 0 at the start, two cultures per SC type were treated with a medium exchange obtaining the referring coculture medium ($2 \times 4 = 8$ monocultures), another two cultures per SC type were seeded with EC in a desired density of 100 cells/mm^2 ($2 \times 4 = 8$ cocultures). To evaluate possible differences of EC characteristics in co- and monoculture, we also seeded two EC monocultures (density: 100 cells/mm^2) in all of the three different specific coculture media ($2 \times 3 = 6$ cultures). Cell cultures were fixed after 24 h (Day 1) and after 48 h (Day 2). For fixation cells on slides were washed two times in phosphate-buffered saline (PBS). After incubation in 0.05 mol/L KCl, cells were fixed with −20°C cold methanol$_{abs}$ in an ice bath. Subsequently, slides were covered with PBS/glycerin (1:10) and stored at −20°C until immunocytochemical staining. In parallel to sample fixation, cell culture supernatants were collected and stored at −80°C to acquire benchmarks of cytokine release by enzyme-linked immunosorbent assay (ELISA).

Thus, each of the HD and UHD experiments required 22 cultures and was done in quadruplicate, so that the resulting number of samples which underwent immunocytochemical staining, quantitative microscopy and ELISA was 22 (slide cultures) × 2 (HD + UHD) × 4 (repetitions) = 176.

In a Conditioning setup, we separately analyzed potential paracrine effects of the SC types on the cytokine release of EC. Therefore, all SC types were seeded in the specific media 48 h before the start with a density of 100 cells/mm^2. After 24 h, medium was switched to coculture medium, which then was conditioned by the individual SC types for exactly 24 h. At Day 0, identical EC cultures, which were prepared 24 h before with a cell density of 100 cells/mm^2, were exposed to the conditioned media (4 ml per slide). Another part of the conditioned media was stored for VEGF, MCP-1, and IL-6 quantification by ELISA. After 24 h (Day 1) and 48 h (Day 2) EC cultures were fixed and medium supernatants were collected for ELISA. As controls, supernatants from parallel EC cultures with nonconditioned coculture medium, which had been placed in the incubator for 24 h instead of conditioning by the SC types, were used. The calculation of the MCP-1 and IL-6 release by EC monocultures in response to SC conditioned media (over- and under-production compared to controls) was done as follows: From the measured MCP-1/IL-6 amount, we first subtracted the cytokine amount introduced by SC conditioned media. Then we subtracted the expected production of MCP-1/IL-6 by EC (cell number corrected release in control cultures with nonconditioned media). Resulting values were then related to the specific number of EC in the cultures fed with SC conditioned media.

2.2 | Immunocytochemical staining

After immunostaining, different cell types in the cocultures were discriminated into von Willebrand factor (vWF)-positive EC (rabbit anti-vWF, 1:500 in PBS/bovine serum albumin 0.1%, no. 12880; Dianova) and vWF-negative SC. The latter were discriminated into α-SMA-positive cells (mouse anti-α-SMA, 1:800, no. A2547, RRID: AB_476701; Sigma), having undergone myofibroblastoid differentiation, and into α-SMA-negative SC. In addition, we identified the rate of cycling cells (outside the phase of cell cycle arrest at G0) by using a Ki-67 mouse antibody (anti-Ki-67/MIB-1, no. N1633; Dakocytomation).

Immunocytochemical staining was carried out according to a standardized protocol.[29] In brief, samples were washed in PBS/0.5% Tween® 20, then incubated with the vWF antibody,

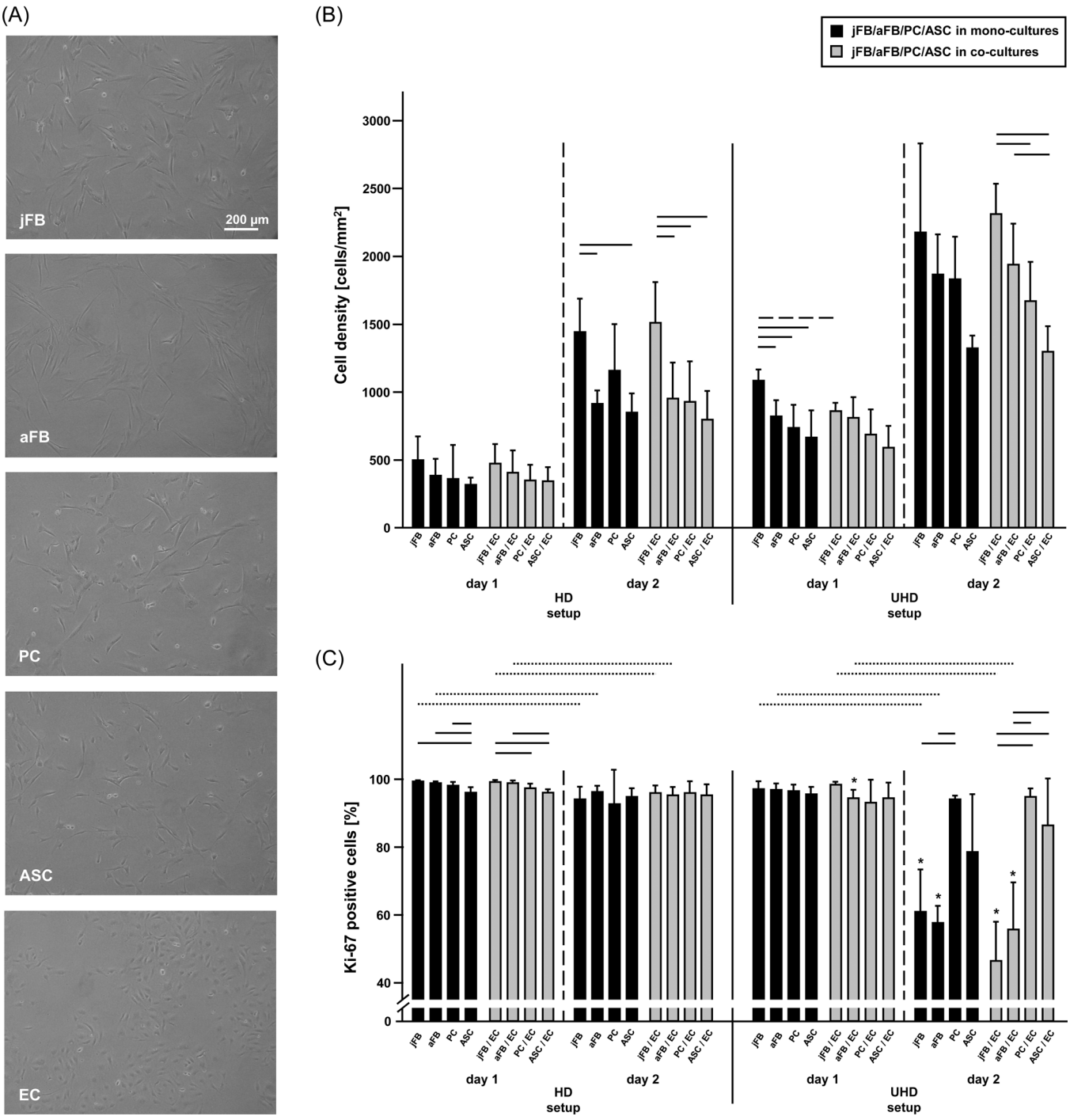

FIGURE 1 Different types of stromal cells (SC) show characteristic cell morphology and proliferation. (A) Phase contrast photomicrographs with typical cell morphologies of SC and endothelial cells (EC) during cell expansion. (B) Cell density assessment of SC in mono- and coculture with EC for culture Days 1 and 2 in the high density (HD) and the ultrahigh density (UHD) setup ($n = 4$, mean values with SD) reveals good proliferation of all SC types and their general tolerance of EC in coculture. Continuous lines indicate significant differences between SC types, broken lines indicate significant differences between mono- and cocultures ($p < .05$). (C) Rate of Ki-67-positive SC in mono- and in coculture with EC ($n = 4$, mean values with SD) again shows the general tolerance of EC in coculture, accompanied by a general reduction of cycling cells among juvenile human fibroblasts (jFB) and adult human fibroblasts (aFB) on Day 2 in the UHD setup. Continuous lines indicate significant differences between SC types, broken lines indicate significant differences between mono- and cocultures, dotted lines indicate significant time-dependent differences, and asterisks indicate significant differences compared to the referring group in the HD setup ($p < .05$).

followed by additional washes and the application of the second antibody (Cy3™-conjugated goat anti-rabbit, 1:200, no. 111-166-045; Dianova). After washing, the α-SMA antibody was applied on one half of the slide and the Ki-67 antibody on the other half. Subsequent to an additional washing both antibodies were detected by AlexaFluor488™ (1:50, no. 115-545-003, RRID: AB_2338840; Jackson Immuno Research Laboratories).

After washing and fixation in 4% paraformaldehyde (in PBS) followed by another washing, samples went through an ascending ethanol series (70%–80%–96% [v/v]). After air-drying, cells were covered with a medium containing 4′,6-diamidino-2-phenylindole (Antifade-DAPI, RRID: AB_2336790, Vectashield; Vector Laboratories) to counterstain the nuclei and preserve the samples. Samples were stored at 4°C until quantitative microscopy.

2.3 | Quantitative microscopy

An Axioskop 2 (Carl Zeiss Microscopy GmbH) and the Axiovision software (RRID: SCR_002677, version 4.2.) were used to analyze the blinded samples. Cell counting of EC and SC on 40 fields of view enabled the calculation of population densities in all cultures fixed at Days 1 and 2. Furthermore, percentage of Ki-67-positive EC and SC as well as percentage of α-SMA-positive SC were determined. Immunostained samples were also used to evaluate cell morphology and cell type arrangement patterns in a qualitative way.

2.4 | ELISA

Cell culture supernatants from each group of mono- and cocultures were pooled ($n = 4$) in the HD and UHD setup, before concentrations of MCP-1 and VEGF were determined. In the Conditioning setup, all supernatants ($n = 4$) from SC monocultures were analyzed separately for VEGF, MCP-1, and IL-6. In addition, the effect of these conditioned media on the release of MCP-1 and IL-6 among EC monocultures was quantified.

Cytokine concentrations were determined by using the referring Quantikine ELISA Human kits (R&D systems) according to the manufacturer's instructions (VEGF: cat. DVE00, RRID: AB_2800364, minimum detectable dose [MDD] < 5.0 pg/ml; MCP-1: cat. DCP00, mean MDD 1.7 pg/ml; IL-6: cat. D6050, MDD < 0.70 pg/ml). We measured absorbance by a microplate reader (Infinite M200; Tecan Deutschland GmbH) and calculated cytokine concentrations by Magellan™ Software (V 7.2., Tecan) using a standard curve. Because cell numbers of all samples were available from quantitative microscopy, we calculated the relative cytokine release per 10e6 cells for each sample.

2.5 | Statistical analysis

To verify statistical differences between different SC types, analysis of variance (ANOVA) with post hoc test (Student–Newman–Keuls) was applied with $p < .05$. For the comparison of two groups (such as the same group in mono- vs. coculture, on Day 1 vs. Day 2, in HD vs. UHD) a Students' t-test was used ($p < .05$). In case of non-given normality or equal variance of the data, ANOVA on ranks or Mann–Whitney rank sum test were applied, respectively.

3 | RESULTS

3.1 | Stromal cell proliferation (cell density)

Cell densities of the different SC types on Day 1 were homogeneous in the HD and the UHD setup (Figure 1B). Only jFB showed a significantly higher initial cell density in the monoculture of the UHD setup, followed by generally high densities on Day 2. An overall weaker cell density was present among ASC, whereas aFB and PC values mostly ranged between the aforementioned cell types.

The SC types tolerate the presence of the EC in coculture. A negative influence of EC on SC proliferation in terms of reduced cell density was only present in a single case: jFB density in the UHD setup was reduced on Day 1.

3.2 | Stromal cell proliferation (cycling cells)

By the quantification of Ki-67-positive cycling cells within a population, we were able to analyze proliferation of SC and the influence of EC in more detail (Figure 1C). In general, cycling cells were detected with a higher percentage for jFB and a lower one for ASC on Day 1 of the HD setup. In the UHD setup on Day 2, where all cell cultures had the highest density, percentages of cycling jFB and aFB were reduced compared to those in the HD setup, both in mono- as well as in coculture. In contrast, PC and ASC still showed high values of cycling cells at high density at Day 2 of the UHD setup.

All SC types tolerate the presence of the EC and were basically not influenced with respect to their stable characteristic proliferation nature.

3.3 | Myofibroblastoid differentiation (α-SMA-positive cells) among stromal cell types

To verify a tissue contraction and vessel stabilizing function of the SC types, we determined the rate of myofibroblastoid cells present within each population, again also focusing on the influence of EC.

We detected a clear ranking with respect to the percentage of myofibroblastoid cells (Figure 2): PC showed the highest percentage of differentiated cells followed by both FB types. However, an additional difference in the rate could be seen between jFB and aFB in the HD setup, where aFB showed higher rates in monoculture.

In general, ASC was the cell type with the lowest rate of myofibroblastoid cells. Nevertheless, ASC was the only cell type

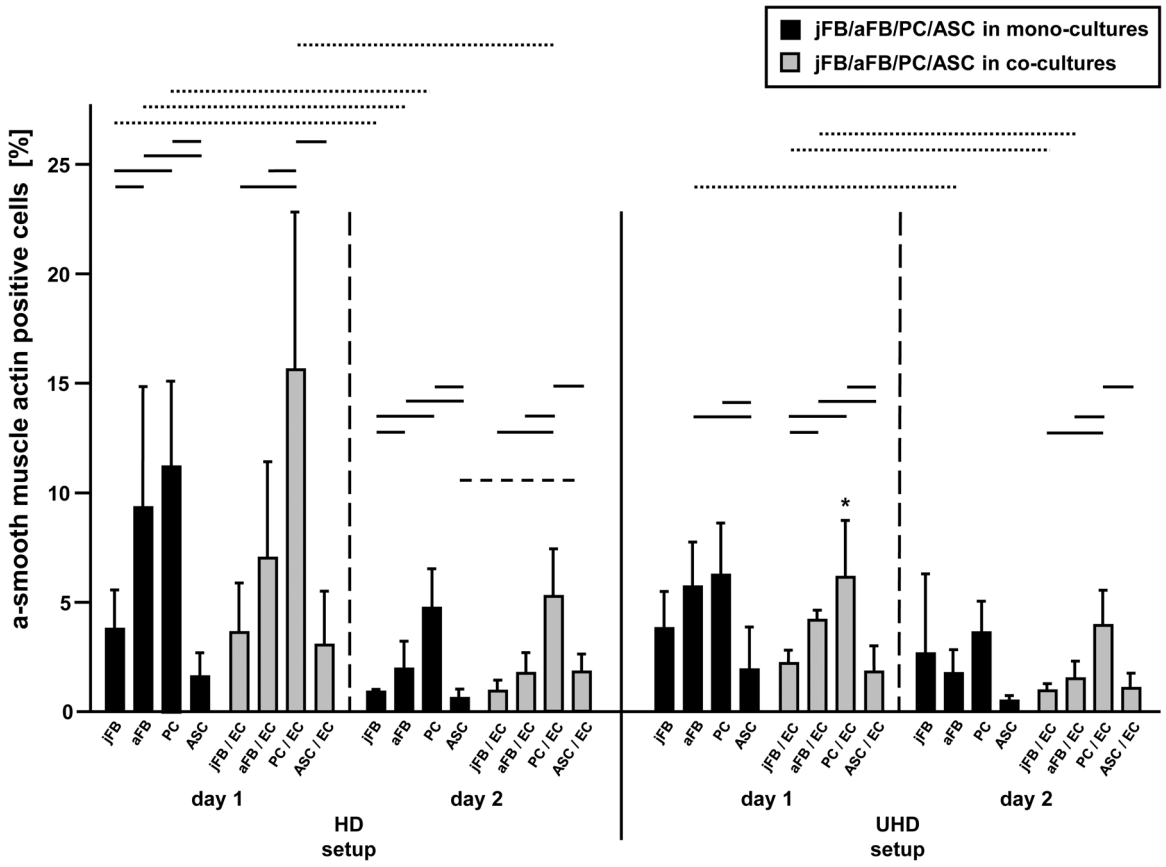

FIGURE 2 Differentiation to a myofibroblastoid cell type among stromal cells (SC) indicates high rates for pericytes (PC) and low, but stable rates for adipose-derived stem cells (ASC). Myofibroblastoid differentiation is indicated by the number of α-smooth muscle actin (α-SMA)-positive SC in % of all SC in mono- and in coculture with EC for culture Days 1 and 2 in the high density (HD) and the ultrahigh density (UHD) setup ($n = 4$, mean values with SD). Continuous lines indicate significant differences between SC types, broken lines indicate significant differences between mono- and cocultures, dotted lines indicate significant time-dependent differences, and asterisks indicate significant differences compared to the referring group in the HD setup ($p < .05$).

responding to EC contact with an increase in the rate of α-SMA-positive cells (on Day 2 of the HD setup). A further extraordinary attribute of ASC was a certain stability of the rates of α-SMA-positive cells over time, while all other cell types were characterized by the reduction of high levels to lower levels up to Day 2.

3.4 | Microvascular endothelial cell adhesion and proliferation (cell densities)

After SC were analyzed in detail in the first part of the results, a detailed characterization of the EC in terms of initial adhesion, their proliferation in monoculture and the effect of the SC in cocultures are displayed in the following.

Despite identical seeding densities, EC density in coculture was often lower than in monoculture, especially in contact with jFB and aFB under all conditions and in contact with PC on Day 2 (Table 1). In contrast, PC and ASC on Day 1 did not affect the EC adhesion, consequently offering best conditions among all SC types.

There was a general proliferation of EC in terms of cell density increase up to Day 2 in the monocultures, but EC proliferation was missing among all different cocultures. However, at least jFB and PC allowed the persistence of the initial EC densities in coculture up to Day 2, which can be interpreted as a stabilizing effect induced by these cells.

3.5 | Microvascular endothelial cell adhesion (percentage in coculture)

The percentage of EC delivered detailed information on their adhesion capability in dependence on the different SC types in coculture (Figure 3A).

With respect to the HD setup, there were no SC type dependent differences in EC percentages. The trend towards a decreasing EC percentage up to Day 2 was already apparent in the HD setup and was confirmed by significance in the UHD setup. The general trend of higher EC percentages in the HD setup was underlined by significance in the coculture with PC at Day 2.

TABLE 1 PC notably support EC adhesion (cell density at Day 1) and persistence (stabilized cell density from Days 1 to 2).

		EC in monoculture	EC in coculture (jFB/EC)	EC in monoculture	Ec in coculture (aFB/EC)	EC inmonoculture	EC in coculture (PC/EC)	EC in monoculture	EC in coculture (ASC/EC)
HD setup cell density (cells/mm^2)	Day 1	66 (±6)[a]	40 (±11)	66 (±6)[a]	52 (±6)	75 (±22)	81 (±27)	59 (±6)	55 (±22)
	Day 2	105 (±17)[a,b]	47 (±22)[c]	105 (±17)[a,b]	43 (±11)	126 (±21)[a,b]	82 (±27)[d]	99 (±35)	47 (±30)
UHD setup cell density (cells/mm^2)	Day 1	74 (±22)[a]	36 (±7)	74 (±22)[a]	42 (±13)	65 (±18)	56 (±12)	61 (±16)	56 (±19)
	Day 2	139 (±41)[a,b]	37 (±18)[c]	139 (±41)[a,b]	36 (±14)	149 (±10)[a,b]	60 (±19)[d]	107 (±27)[a,b]	50 (±20)

Note: Cell densities of EC in mono- and in coculture with SC for culture Days 1 and 2 in the HD and the UHD setup ($n = 4$, mean values with SD).

Abbreviations: aFB, adult human fibroblasts; ASC, adipose-derived stem cells; EC, endothelial cells; HD, high density; jFB, juvenile human fibroblasts; PC, pericytes; SC, stromal cells; UHD, ultrahigh density.

[a]Significant versus cell density in the referring cocultures ($p < .05$).

[b]Significant versus cell density in the referring Day 1 cultures ($p < .05$).

[c]Cocultures potentially stabilizing endothelial cells from Day 1 to Day 2.

Highest EC percentages were detected in coculture with PC and ASC in the HD setup, again indicating that PC and ASC are the most supporting SC types for EC adhesion. Furthermore, ASC allowed a significantly high percentage of EC at Day 1 in the UHD setup.

3.6 | Microvascular endothelial cell proliferation (cycling cells)

The levels of cycling EC in coculture (Figure 3B) were not influenced by the different cell densities in the HD and UHD setup, with only one exception: The general trend of high percentages of cycling EC in coculture with PC was underlined by significance on Day 1 in the HD setup. In addition to PC, ASC tendentiously allowed a better EC cycling, reaching significance, when ASC densities were highest at Day 2 of the UHD setup.

In conclusion, the data on EC percentage and cycling in coculture, although impeded by high standard deviation in some cases, indicate a more beneficial milieu for EC provided by PC and ASC compared to a more unfavorable milieu offered by both FB types. In detail, PC seem to be beneficial rather at lower cell densities, whereas ASC might be more beneficial at high densities.

3.7 | Cytokine release of stromal cells in the HD and UHD setup: VEGF, MCP-1

To acquire benchmarks for the release of paracrine factors among SC, we quantified VEGF and MCP-1 in cell culture supernatants on Days 1 and 2 in the HD and UHD setup by pooling the samples of four repetitions from identical monocultures (Table 2). PC released VEGF moderately in both setups only on Day 2, whereas ASC generally secreted VEGF in high amounts. aFB released VEGF under each condition at low levels. Among jFB, VEGF was only detectable at a low level in the HD setup on Day 1.

In both setups a solid MCP-1 release could be detected among PC and jFB, whereas aFB showed lower levels. MCP-1 release of ASC ranged in between, increasing up to Day 2.

As it is not possible to assign measured cytokine values to the individual cell type, either SC or EC, in coculture, we additionally launched a Conditioning setup delivering reliable data concerning the paracrine signaling impact of SC on the MCP-1 and IL-6 release of EC.

3.8 | Cytokine patterns of stromal and microvascular endothelial cells in the Conditioning setup: VEGF, MCP-1, IL-6

VEGF release among the SC types during conditioning were comparable to those in the HD and UHD setup: PC initially did not release detectable amounts of VEGF, whereas ASC showed the highest mean VEGF value (Figure 4A). jFB and aFB exhibited similar values ranging below those for ASC.

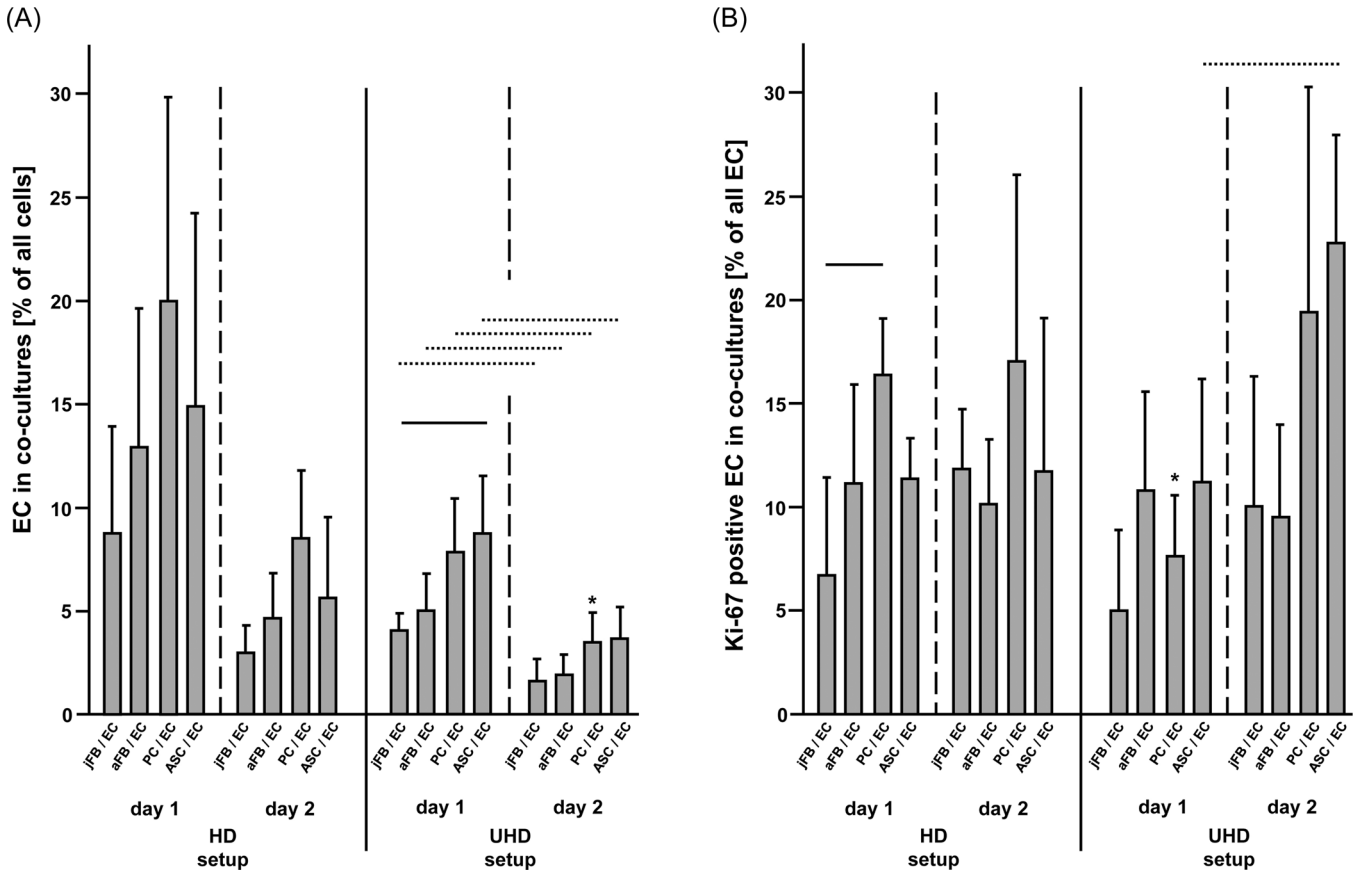

FIGURE 3 Pericytes (PC) and adipose-derived stem cells (ASC) provide a favorable milieu for endothelial cells (EC) in terms of adhesion, persistence, and cycling. (A) Adhesion of EC (Day 1) and persistence of EC (Day 2) indicated by the fraction of EC in relation to total cells in cocultures with SC in % ($n = 4$, mean values with SD). (B) Rate of Ki-67-positive EC in coculture with SC ($n = 4$, mean values with SD). Continuous lines indicate significant differences between cultures, dotted lines indicate significant time-dependent differences, and asterisks indicate significant differences compared to the referring group in the high density (HD) setup ($p < .05$).

TABLE 2 Characteristic cytokine release of different SC types in monoculture, revealing high levels of VEGF among ASC and high levels of MCP-1 among PC and jFB.

		HD setup jFB	HD setup aFB	HD setup PC	HD setup ASC	UHD setup jFB	UHD setup aFB	UHD setup PC	UHD setup ASC
VEGF (ng/10e6 cells)	Day 1	0.07	0.28	n.d.	1.68	n.d.	0.16	n.d.	2.83
	Day 2	n.d.	0.29	0.38	2.23	n.d.	0.10	0.65	4.17
MCP-1 (ng/10e6 cells)	Day 1	1.88	0.30	2.01	0.39	2.32	0.42	2.00	0.80
	Day 2	1.32	0.27	1.59	0.47	1.82	0.20	1.89	1.55

Note: Mean concentrations (ng/10e6 cells) of VEGF and MCP-1 in supernatants of SC monocultures for culture Days 1 and 2 in the HD and the UHD setup ($n = 4$, pooled).

Abbreviations: aFB, adult human fibroblasts; ASC, adipose-derived stem cells; HD, high density; jFB, juvenile human fibroblasts; MCP-1, monocyte chemoattractant protein-1; n.d., not detectable; PC, pericytes; SC, stromal cells; UHD, ultrahigh density; VEGF, vascular endothelial growth factor.

In contrast, jFB and aFB released different amounts of MCP-1 into the medium, with jFB presenting the highest values overall. In addition, and comparable to the HD and UHD setup, PC were characterized by a solid release of MCP-1, whereas aFB and ASC ranged at lower levels.

The overall MCP-1 release pattern was similar to the release pattern of IL-6, where aFB and ASC showed a weaker release compared to jFB and PC, the latter exhibiting the highest IL-6 value.

Subsequent to the exposure of identical EC cultures to SC conditioned media and to unconditioned media (control cultures),

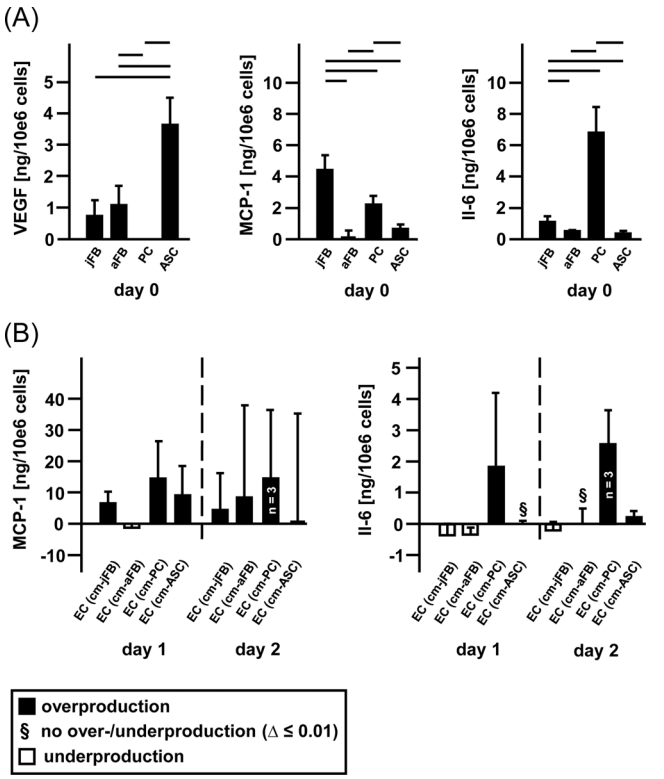

FIGURE 4 Cytokine release of individual types of stromal cells (SC) is characteristic and provokes an individual reaction among endothelial cells (EC). (A) SC conditioned media before transfer to EC ($n = 4$, mean values with SD, $p < .05$). Continuous lines indicate significant differences between cultures. (B) Cytokine release (over- and underproduction) by EC monocultures in response to SC conditioned media (cm) ($n = 4$ each unless given otherwise, mean values with SD).

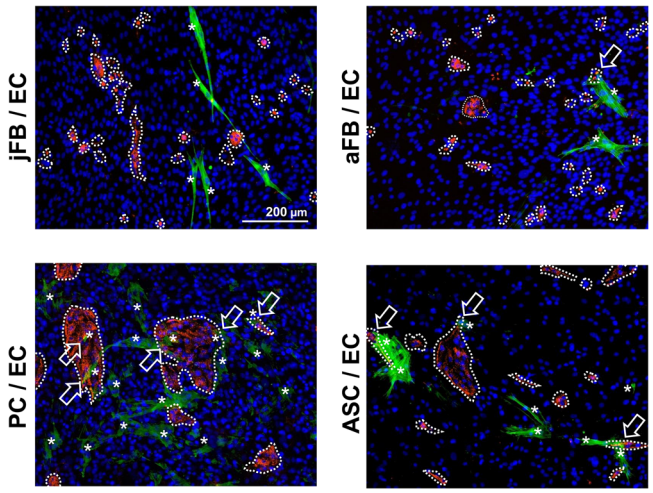

FIGURE 5 Local cell arrangement and interaction with endothelial cells (EC) reveal adipose-derived stem cells (ASC) as the most versatile type of stromal cells (SC). Fluorescence photomicrographs showing patterns of EC positive for von Willebrand factor (encircled by broken lines) and α-smooth muscle actin (α-SMA) expressing myofibroblastoid cells (indicated by asterisks) in ultrahigh density cocultures of EC with SC. SC without α-SMA expression are visible as nuclei only. Regions of directly interacting SC and EC are indicated by arrows.

we were able to estimate, whether the paracrine EC response to SC either results in over- or underproduction of MCP-1 and IL-6. EC responded to all conditioned media by an enhanced release of MCP-1, except to aFB-derived medium, where a decreased release was detected on Day 1 (Figure 4B). MCP-1 release by EC in response to ASC conditioned medium at Day 2 was quite heterogeneous, resulting in low mean values. The maximum MCP-1 release among EC was detected as a response to media conditioned by PC.

Comparable to this behavior, IL-6 was generally strongly released as a response to PC conditioned media, too. Apart from PC conditioned media, just ASC conditioned media allowed a weak additional release of IL-6 by EC at Day 2. Media from jFB and aFB generally provoked an IL-6 underproduction.

3.9 | Stromal and microvascular endothelial cell patterns

The general layout of the 2D cell culture experiments by first seeding the SC followed by addition of EC 48 h later allowed us to evaluate, whether typical arrangement patterns of SC and EC develop during adhesion and interaction.

Although a certain heterogeneity of identical cultures within the experimental repetitions impeded quantification, especially the UHD setup offered the opportunity to identify EC arrangement patterns. We also focused on the appearance of myofibroblastoid cells in the individual SC types and their contact to EC (Figure 5).

Whereas PC and ASC allowed EC arrangement in typical clusters, those clusters, if present at all, were smaller in both cocultures with FB. In both FB cocultures myofibroblastoid cells lacked intensive contact to EC and their morphological appearance differed: Whereas jFB showed extensively elongated shaped myofibroblastoid cells, there was a larger and more sheet like type detectable among aFB.

In the PC and ASC cocultures, EC were sometimes locally accompanied by myofibroblastoid cells. Myofibroblastoid ASC manifested either with a sheet like morphology or with elongated shape. Myofibroblastoid ASC with elongated shape showed the power to initiate an elongated orientation of EC, indicating a guidance function. Myofibroblastoid PC in cocultures showed a more compact α-SMA pattern and seemed not to have an influence on EC orientation or guidance.

4 | DISCUSSION

In a developing functional granulation tissue, cell density increases in a spatiotemporal order. Current in vitro models often lack a sophisticated analysis to correlate cell density with cell function.

Although quite similar characteristics of the SC types were observed in the HD and the UHD setup, the detailed comparison of the results delivers additional information for future improvement of soft tissue healing assessment and therapy.

In our model, we decided on a "joint-nutrition" with coculture medium (one part of the individual SC medium and one part of ECG) to offer a common baseline for proliferation of each SC type according to its individual needs. While cell proliferation was present among all SC types, jFB presented highest cell numbers at the different points in time. Both jFB and aFB showed high numbers of cycling Ki-67-positive cells in the beginning. This special talent for early proliferation might underscore the important role of FB during granulation tissue formation in vivo.[30] In contrast, PC and ASC maintained high numbers of cycling cells in the UHD setup, indicating a more stable proliferation and a better endurance than the FB types. This hints to extraordinary long-term functions of PC and ASC in granulation tissue.

In coculture, EC were tolerated by the SC types, which maintained their characteristic proliferation nature to a large extent, emphasizing their dominant and stable character. However, EC had a dampening effect on the initial density of jFB in the UHD setup. Vice versa the results illustrate how EC are likely influenced by the different SC in the context of regulating angiogenesis and granulation tissue formation.[7] There was a sophisticated attraction potential of each SC type on EC in our model: Initial EC adhesion in coculture was highest in contact with PC, accompanied by an EC stabilizing effect over time. Transferred to the in vivo situation we can assume a high binding efficiency of PC by cell-to-cell contacts and extracellular matrix proteins, correlating to the vessel stabilization function of PC.[19] Similarly, such a function was offered by ASC, too, due to the good initial adhesion of EC. A certain EC stabilizing effect was detectable among jFB in terms of persisting EC densities in cocultures over time, pointing to a potential function of FB as mural cells of microvessels in vivo.

Proliferation of EC is a prerequisite for angiogenesis related vascular sprouting.[12] Whereas both FB types seemed to offer a more unfavorable milieu, proliferation in terms of cell cycling of EC in coculture was assured in a milieu provided by PC and ASC. PC seem to permit proliferation of EC especially at moderate cell densities. ASC allow EC cycling even at high densities, maybe indicating that ASC in vivo permit both concurring processes, angiogenesis and vessel stabilization, in parallel for longer periods and at high cell densities. In addition, just PC and ASC allowed the typical cluster arrangement of EC, while both FB types only allowed small clusters with a limited number of EC.

To evaluate in more detail the stabilizing nature of the SC types—both in the context of vessel stabilization and granulation tissue contraction—we characterized myofibroblastoid differentiation. Myofibroblastoid differentiation among ASC ranged at low, but stable levels. In addition, ASC were the only SC type responding significantly to EC contact in coculture by increased myofibroblastoid differentiation. α-SMA-positive ASC appeared as (i) elongated cells with contact to EC, indicating a guidance function during vessel development in vivo, and as (ii) large, sheet-like cells without contact to EC, indicating their participation in tissue contraction.[24]

Among PC, the good availability of myofibroblastoid cells highlights their function in tissue contraction[31] and vessel stabilization.[23] Indeed PC had direct contact to EC, confirming a good vessel stabilizing function. This cell-to-cell contact underlines the in vivo potential of PC to regulate the vascular diameter of capillaries due to contractile functions.[12] In addition, contractile changes in PC can contribute to capillary disfunction and shunting.[13] However, PC did not have a detectable influence on EC orientation and α-SMA-positive PC mainly appeared in a compact cell shape, so that a guidance function during angiogenesis seems not to be likely. Thus, PC movement away from the vessel site in vivo could allow angiogenesis in a granulation tissue first, while, after maturation, higher PC densities could account for microvessel stabilization[12] and regulation of the microvascular tone.[14]

jFB showed a low rate of myofibroblastoid cells together with absent EC contact, leading to the assumption that they play a secondary role in vessel stabilization. aFB showed higher rates of myofibroblastoid cells but were also lacking intensive contact to EC, so that a vessel supporting function is unlikely, too. Among aFB, the high number of more sheet-like α-SMA-positive cells with a large surface is rather linked to an enhanced presence of a senescent phenotype[32] than to tissue contraction.

aFB were also different from jFB with respect to their cytokine release: jFB showed higher release of MCP-1 and IL-6, as well as an early release of VEGF in weak amount, indicating an angiogenesis stimulating effect rather in the early phase of tissue repair by simultaneously providing proangiogenic VEGF and proinflammatory MCP-1 and IL-6.[11] aFB were characterized by a weak release of MCP-1, IL-6, and VEGF. In addition, aFB derived medium caused an early MCP-1 underproduction among EC. These results support the assumption, that aFB are not able to initiate early inflammation necessary to trigger angiogenesis.

PC released both MCP-1 and IL-6 in constantly high amounts and additionally provoked the overproduction of just these cytokines by EC. The interpretation of these results with respect to a proangiogenic function of PC in vivo indicates, that they initially act by assuring an inflammatory milieu, followed by the provision of VEGF later on. However, vessel stabilization during maturation by releasing and provoking high levels of MCP-1 and IL-6 as another potential function of PC[33] is also indicated by the given results.

ASC provided high amounts of VEGF in combination with moderate amounts of MCP-1 and IL-6. ASC conditioned medium caused a moderate overproduction of MCP-1 and IL-6 by EC on Day 2. This special character of ASC, to deliver VEGF and to regulate the MCP-1 and IL-6 balance, could be important to enable EC proliferation, as it was detectable at Day 2 of the setup by best Ki-67 rates. At this very time ASC were able to stabilize the myofibroblastoid population. Thus, ASC seem to support both proliferation of EC necessary for angiogenesis as well as EC stabilization during vessel maturation. Both features were reflected in the morphology of the ASC/EC cocultures, where EC proliferation

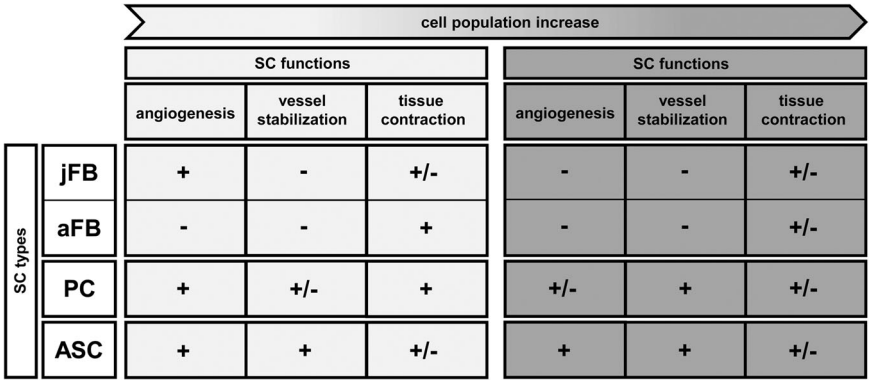

FIGURE 6 Future tissue repair concepts might profit especially from pericytes (PC) and adipose-derived stem cells (ASC). Potential functions (+: strong effect, +/−: moderate effect, −: weak effect) of different types of stromal cells (SC) in a granulation tissue revealed by the present in vitro study. A cell population increase is indicated by the comparison of high density (HD) setup data with ultrahigh density (UHD) setup data and by the comparison of Day 1 data with Day 2 data.

in clusters was possible, but elongated EC guided by myofibroblastoid ASC were detectable, too. In vivo, the invasion of ASC from the niche in to the granulation tissue as well as the autologous donation of ASC thus might lead to the optimization of tissue repair.

5 | CONCLUSION

The 2D model applied in this study confirmed individual characteristics of the SC types indicated by preceding studies. Beyond that, the model was successful for the identification of additional density-dependent characteristics, which are especially important in the context of a dynamic granulation tissue. The detailed view on cell morphology, (self-) organization and on cell functions (apparent in cytokine regulation and cell interaction) discloses a new in vitro perspective for a better understanding of in vivo soft tissue healing. Future strategies including 3D approaches,[34] enhanced sample sizes of individual primary SC types as well as a deeper focus on the relevance of the donor age of autologous SC will stimulate the development of new diagnostic tools and advanced therapies for soft tissue healing.

At the current stage the results disclosed characteristic properties of rivaling SC types in a granulation tissue, which are summarized in Figure 6: Both FB types showed an early and later on decreasing proliferation and seemed not to have a main function in vessel stabilization, but rather play a role in tissue stabilization[35] and contraction[21,22] by providing myofibroblastoid cells. The early function of jFB, delivering VEGF and providing a proinflammatory milieu, leads to the assumption, that angiogenesis profits from jFB at early stages. Such a function was lacking in the case of aFB maybe correlating to a beginning senescence. PC showed a different behavior: Cytokine release, long-term proliferation, myofibroblastoid differentiation, and allowance of EC cluster arrangement indicated main functions in angiogenesis and vessel stabilization during all stages of repair. These processes are likely regulated via cell density with angiogenesis favored at lower cell densities and vessel stabilization favored at higher cell densities. Indeed, ASC appeared as the most versatile SC type, because proangiogenic, immunomodulatory and stabilizing functions seem to be available independent from cell density.

In summary, a limited potential might be expected for FB with respect to their application in tissue repair concepts whereas a promising role for PC and ASC is indicated. However, every approach to use mesenchymal stem cells in regenerative medicine has to consider their potential to transform into cancer cells,[27] until more reliable data are available.

ACKNOWLEDGMENT

Open Access funding enabled and organized by Projekt DEAL.

CONFLICT OF INTEREST

The authors declare no conflict of interest.

DATA AVAILABILITY STATEMENT

There is no other data available for this article. All the data have been used in the figures.

ORCID

Martin Oberringer http://orcid.org/0000-0002-9476-986X

REFERENCES

1. Lindholm C, Searle R. Wound management for the 21st century: combining effectiveness and efficiency. *Int Wound J*. 2016;13(suppl 2):5-15. doi:10.1111/iwj.12623
2. Diegelmann RF, Evans MC. Wound healing: an overview of acute, fibrotic and delayed healing. *Front Biosci*. 2004;9:283-289. doi:10.2741/1184
3. Greenhalgh DG. The role of apoptosis in wound healing. *Int J Biochem Cell Biol*. 1998;30(9):1019-1030. doi:10.1016/s1357-2725(98)00058-2
4. Hassan WU, Greiser U, Wang W. Role of adipose-derived stem cells in wound healing. *Wound Repair Regen*. 2014;22(3):313-325. doi:10.1111/wrr.12173
5. Ichim TE, O'Heeron P, Kesari S. Fibroblasts as a practical alternative to mesenchymal stem cells. *J Transl Med*. 2018;16(1):212. doi:10.1186/s12967-018-1536-1

6. Bodnar RJ, Satish L, Yates CC, Wells A. Pericytes: a newly recognized player in wound healing. *Wound Repair Regen*. 2016;24(2):204-214. doi:10.1111/wrr.12415
7. Hu MS, Borrelli MR, Lorenz HP, Longaker MT, Wan DC. Mesenchymal stromal cells and cutaneous wound healing: a comprehensive review of the background, role, and therapeutic potential. *Stem Cells Int*. 2018;2018:6901983. doi:10.1155/2018/6901983
8. Gillitzer R, Goebeler M. Chemokines in cutaneous wound healing. *J Leukoc Biol*. 2001;69(4):513-521.
9. Ridiandries A, Tan JTM, Bursill CA. The role of chemokines in wound healing. *Int J Mol Sci*. 2018;19(10):3217. doi:10.3390/ijms19103217
10. Johnson BZ, Stevenson AW, Prêle CM, Fear MW, Wood FM. The role of IL-6 in skin fibrosis and cutaneous wound healing. *Biomedicines*. 2020;8(5):101. doi:10.3390/biomedicines8050101
11. Kwon HM, Hur SM, Park KY, et al. Multiple paracrine factors secreted by mesenchymal stem cells contribute to angiogenesis. *Vascul Pharmacol*. 2014;63(1):19-28. doi:10.1016/j.vph.2014.06.004
12. Van Dijk CG, Nieuweboer FE, Pei JY, et al. The complex mural cell: pericyte function in health and disease. *Int J Cardiol*. 2015;190:75-89. doi:10.1016/j.ijcard.2015.03.258
13. Erdener ŞE, Dalkara T. Small vessels are a big problem in neurodegeneration and neuroprotection. *Front Neurol*. 2019;10:889. doi:10.3389/fneur.2019.00889
14. Kutcher ME, Herman IM. The pericyte: cellular regulator of microvascular blood flow. *Microvasc Res*. 2009;77(3):235-246. doi:10.1016/j.mvr.2009.01.007
15. Wong VW, Levi B, Rajadas J, Longaker MT, Gurtner GC. Stem cell niches for skin regeneration. *Int J Biomater*. 2012;2012:926059. doi:10.1155/2012/926059
16. Rohringer S, Hofbauer P, Schneider KH, et al. Mechanisms of vasculogenesis in 3D fibrin matrices mediated by the interaction of adipose-derived stem cells and endothelial cells. *Angiogenesis*. 2014;17(4):921-933. doi:10.1007/s10456-014-9439-0
17. Kuwabara JT, Tallquist MD. Tracking adventitial fibroblast contribution to disease: a review of current methods to identify resident fibroblasts. *Arterioscler Thromb Vasc Biol*. 2017;37(9):1598-1607. doi:10.1161/ATVBAHA.117.308199
18. Rey FE, Pagano PJ. The reactive adventitia: fibroblast oxidase in vascular function. *Arterioscler Thromb Vasc Biol*. 2002;22(12):1962-1971. doi:10.1161/01.atv.0000043452.30772.18
19. Bergers G, Song S. The role of pericytes in blood-vessel formation and maintenance. *Neuro Oncol*. 2005;7(4):452-464. doi:10.1215/S1152851705000232
20. Hinz B, Celetta G, Tomasek JJ, Gabbiani G, Chaponnier C. Alpha-smooth muscle actin expression upregulates fibroblast contractile activity. *Mol Biol Cell*. 2001;12(9):2730-2741. doi:10.1091/mbc.12.9.2730
21. Gabbiani G, Hirschel BJ, Ryan GB, Statkov PR, Majno G. Granulation tissue as a contractile organ. A study of structure and function. *J Exp Med*. 1972;135(4):719-734. doi:10.1084/jem.135.4.719
22. Desmoulière A, Darby IA, Gabbiani G. Normal and pathologic soft tissue remodeling: role of the myofibroblast, with special emphasis on liver and kidney fibrosis. *Lab Invest*. 2003;83(12):1689-1707. doi:10.1097/01.lab.0000101911.53973.90
23. Dulmovits BM, Herman IM. Microvascular remodeling and wound healing: a role for pericytes. *Int J Biochem Cell Biol*. 2012;44(11):1800-1812. doi:10.1016/j.biocel.2012.06.031
24. Kakudo N, Kushida S, Suzuki K, et al. Effects of transforming growth factor-beta1 on cell motility, collagen gel contraction, myofibroblastic differentiation, and extracellular matrix expression of human adipose-derived stem cell. *Hum Cell*. 2012;25(4):87-95. doi:10.1007/s13577-012-0049-0
25. Hinz B. Formation and function of the myofibroblast during tissue repair. *J Invest Dermatol*. 2007;127(3):526-537. doi:10.1038/sj.jid.5700613
26. Gould L, Abadir P, Brem H, et al. Chronic wound repair and healing in older adults: current status and future research. *J Am Geriatr Soc*. 2015;63(3):427-438. doi:10.1111/jgs.13332
27. Lee HY, Hong IS. Double-edged sword of mesenchymal stem cells: cancer-promoting versus therapeutic potential. *Cancer Sci*. 2017;108(10):1939-1946. doi:10.1111/cas.13334
28. Oberringer M, Meins C, Bubel M, Pohlemann T. A new in vitro wound model based on the co-culture of human dermal microvascular endothelial cells and human dermal fibroblasts. *Biol Cell*. 2007;99(4):197-207. doi:10.1042/BC20060116
29. Schwarz F, Jennewein M, Bubel M, Holstein JH, Pohlemann T, Oberringer M. Soft tissue fibroblasts from well healing and chronic human wounds show different rates of myofibroblasts in vitro. *Mol Biol Rep*. 2013;40(2):1721-1733. doi:10.1007/s11033-012-2223-6
30. Greaves NS, Ashcroft KJ, Baguneid M, Bayat A. Current understanding of molecular and cellular mechanisms in fibroplasia and angiogenesis during acute wound healing. *J Dermatol Sci*. 2013;72(3):206-217. doi:10.1016/j.jdermsci.2013.07.008
31. Schuster R, Rockel JS, Kapoor M, Hinz B. The inflammatory speech of fibroblasts. *Immunol Rev*. 2021;302(1):126-146. doi:10.1111/imr.12971
32. Mellone M, Hanley CJ, Thirdborough S, et al. Induction of fibroblast senescence generates a non-fibrogenic myofibroblast phenotype that differentially impacts on cancer prognosis. *Aging*. 2016;9(1):114-132. doi:10.18632/aging.101127
33. Schneider G, Bubel M, Pohlemann T, Oberringer M. Response of endothelial cells and pericytes to hypoxia and erythropoietin in a co-culture assay dedicated to soft tissue repair. *Mol Cell Biochem*. 2015;407(1-2):29-40. doi:10.1007/s11010-015-2451-x
34. Oberringer M, Bubel M, Jennewein M, et al. The role of adipose-derived stem cells in a self-organizing 3D model with regard to human soft tissue healing. *Mol Cell Biochem*. 2018;445(1-2):195-210. doi:10.1007/s11010-017-3265-9
35. Gerarduzzi C, Di Battista JA. Myofibroblast repair mechanisms post-inflammatory response: a fibrotic perspective. *Inflamm Res*. 2017;66(6):451-465. doi:10.1007/s00011-016-1019-x

How to cite this article: Kuhn P, Bubel M, Jennewein M, Guthörl S, Pohlemann T, Oberringer M. Dose-dependent dominance: how cell densities design stromal cell functions during soft tissue healing. *Cell Biochem Funct*. 2022;40:439-450. doi:10.1002/cbf.3705